Africa Journal of Physical Sciences Vol. 8, pp. 103-120, July 2024
http://uonjournals.uonbi.ac.ke/ojs/index.php/ajps
ISSN 2313-3317

Photocatalytic Activity of Semiconductor Oxide, Titanium Dioxide - Tungsten Trioxide Nanocomposite Material in Visible Light

Florence Masese[a]*, Shem O. Wandiga[a], Vincent Madadi[a], Damaris Mbui[a]

[a] Department of Chemistry, University of Nairobi, P.O. Box 30197-00100, Nairobi, Kenya.

* Corresponding author email:maseseflorence15@gmail.com

ARTICLE INFO

Article History:
Received: 22/09/2022
Accepted: 25/10/2023
Available online: 25 July 2024

Keywords:
Mineralization
Recycling
Characterization
Semiconductor
Nanocomposite
Visible radiation

ABSTRACT

A range of recalcitrant organic pollutants are introduced into environment from industrial wastewater causing global water quality risks. The study aimed to investigate the efficacy of synthesized coupled titanium (IV) oxide photocatalysts in the degradation of methylene blue, serving as a model pollutant representative of dyes and recalcitrant organic compounds in water sources. An innovative method was made use of to synthesize a semiconductor oxide, titanium dioxide coupled with tungsten trioxide nanocomposite, at room temperature in molar ratios of 1:1, 1:4, and 4:1. The synthesised nanoparticles were characterised using Brunnauer-Emmett-Teller analysis, X-ray diffraction, Ultra Violet-Visible spectroscopy and Fourier transform infrared. Photocatalytic degradation of methylene blue in aqueous solution under to visible light radiation and the performance of coupled TiO_2/WO_3 nanocomposite were evaluated. The effects of pH, catalyst loading and concentration on degradation of methylene blue was also assessed. Nanocomposite ratio of 1:1, catalystic loading of 0.25g/50 mL and 20 ppm methylene blue solution tested at pH 2 and pH 12 yielded optimal degradation results, with efficiency of 87.8% after 30 minutes exposure to visible light. The degree of mineralization of methylene blue evaluated using closed reflux colorimetric method, yielded 86% organic matter reduction in 3 hours. Reusability of titanium dioxide coupled with tungsten trioxide nanocomposite tested through 4 cycles of treatments using equimolar solutions of methylene blue yielded degradation efficiency of 93%, 90% 88% and 87% for cycles 1, 2, 3 and 4 respectively, suggesting photocatalyst stability and efficiency. Titanium dioxide coupled with tungsten trioxide was successfully synthesized. Under optimal conditions, the photocatalyst degraded 20 ppm of methylene blue. This demonstrates that coupling titanium dioxide with tungsten trioxide enhances the photo-absorption of titanium dioxide, thereby increasing its effectiveness in treating contaminated domestic water.

ISSN 2313-3317

1. Introduction

The world faces a serious problem of environmental degradation due to unsustainable development and poor management of chemicals of diverse nature [1]. The release of

untreated or poorly treated effluents into water systems adversely affect human health and different lifeforms in aquatic systems causing detrimental damage to ecosystems [2]. Water pollution is one of the major causes of inadequate quantity and quality of potable water. Researchers want to create efficient photocatalytic materials that can eliminate contaminants from both air and water. Furthermore, the world's fast-growing population has put enormous pressure on the globe in terms of overexploitation of limited resources and the release of harmful substances into the environment [3]. Due to the increasing accumulation of pollutants in the environment beyond the self-cleaning ability, research in environmental decontamination has received increasing attention. One of the areas attracting research is the development of effective photocatalytic materials for removal of recalcitrant pollutants in air, soil and water [4].

The interest in photocatalysis over the years is due to its ability to purify water and convert various pollutants into environmentally safe byproducts at a low cost [5]. Science-based methods for removing pollutants from the environment have focused on employing semiconductors photocatalysts [6], particularly the use of titanium dioxide since it is readily available, affordable, non-toxic, highly catalytic, stable and possesses strong oxidizing properties [7]. Large deposits of Titanium ores exist in Kwale County, Kenya. However, due to its large band gap (>3.2 eV), its application is limited and active only under UV light, it can only absorb UV radiation which constitutes less than 5% of the solar radiation spectrum [3]. This large band gap barrier restricts photogenerated electrons from photodegradation processes by allowing them to quickly recombine [8]. Whereas the photo-response of titanium dioxide has been investigated in the past under visible radiation using different techniques such as metal ion doping [9], non-metal doping [10], noble metal deposition and composite semiconductors [11] are considered cutting-edge "green" oxidation technology [12] techniques, these methods are expensive for local communities. Therefore, the current research investigated the catalytic performance of TiO_2 with a semiconductor to enhance charge separation and to broaden energy range for photoexcitation [13].

2. Materials and Methods

2.1. Chemicals and reagents

TiO_2 and WO_3 chemicals applied in this study were of high purity of 99.4% and 99.995%, respectively, from Sigma Aldrich. NaF (98.5%) from Thomas Baker Chemicals India, Analytical grade Nitric acid (65% and 68%) from Uni-CHEM chemical reagents, and isopropanol (99.9%) from J.T. Baker's, and methylene blue (MeB) dye (82%) from Loba Chemie. Double distilled water was used in preparation of solutions. The MeB dye structural details are presented in Figure 1, and the absorbance curve in Figure 2 had a maximum wavelength (λ_{max}) at 663.9 nm.

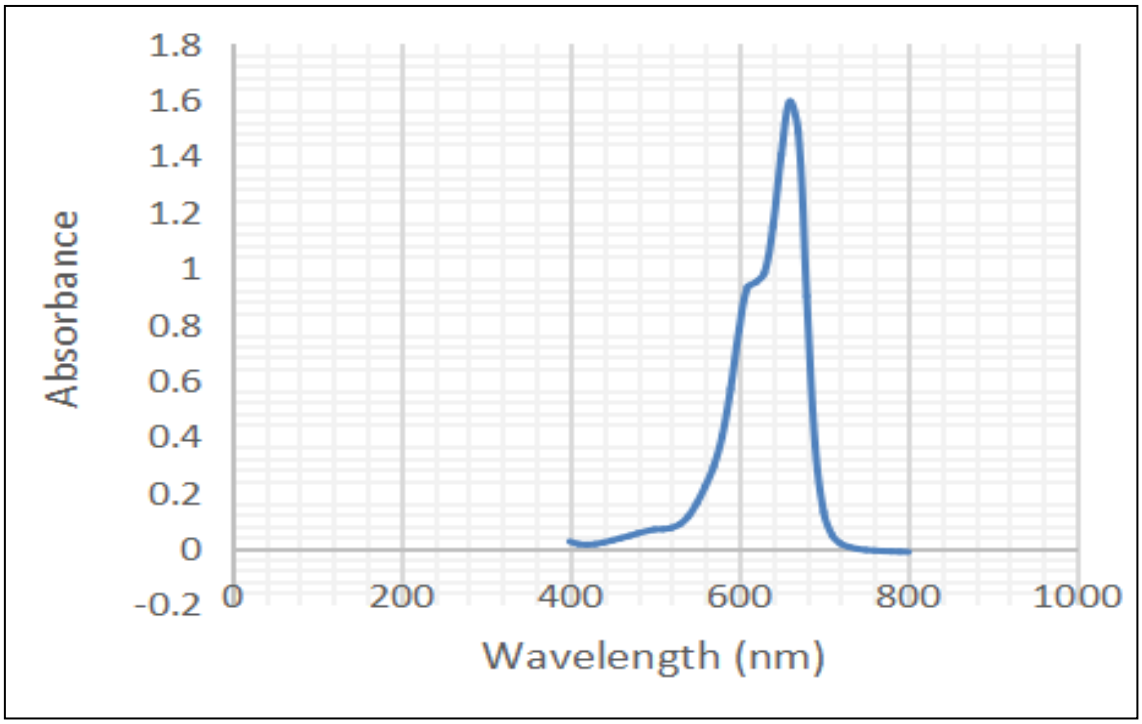

Figure 1: Structure of 3,7-bis(dimethylamino)-phenothiazin-5-ium chloride

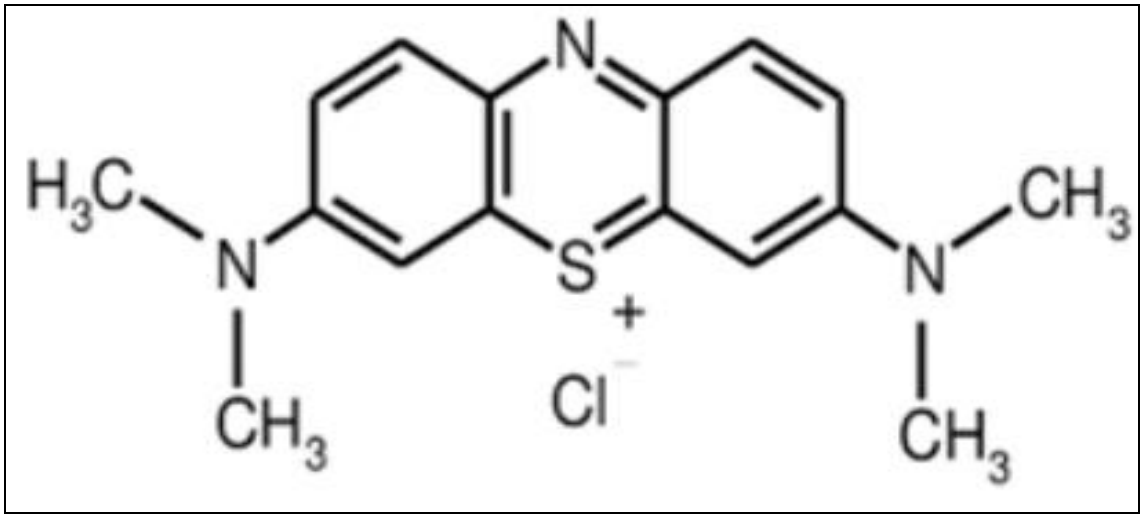

Figure 2. Absorbance curve for methylene blue

2.2. Preparation of titanium (IV) oxide - tungsten (VI) oxide nanocomposite

A novel method for preparing photocatalysts at room temperature was used. TiO_2, WO_3, and NaF were weighed out and combined in a 1:1:2 molar ratio with 40 cm^3 of isopropanol. Nitric acid was used to keep the mixture's pH at 2, and for 12 hours, it was magnetically agitated while exposed to visible light. Using 0.45 µm membrane filter sheets, the precipitate was vacuum-filtered and dried at 110 ^oC overnight. The residues were subsequently calcined for two hours at 575 °C in a muffle furnace.

2.3. Characterization of the photocatalyst

Synthesised coupled semiconductor TiO_2-WO_3 nanocomposite was characterized using X-ray diffraction, Brunnauer-Emmett-Teller (BET), UV/Vis spectroscopy, and Fourier transform infrared spectroscopy. Methylene blue was selected as a representative contaminant for degradation to gauge the photocatalysts' catalytic activity when exposed to visible light. A D2 Phaser 2nd Generation X-Ray diffractometer (Bruker, Germany) at Geology and Mines laboratory Nairobi Kenya was used for characterization. X-ray powder Diffraction (XRD) spectra were captured using Cu-K radiation (wavelength = 0.1541 nm) to ascertain the phase formation and crystallinity of the material. Operating conditions applied followed 30 kV and 10 mA current, with a scan speed of 0.09º step per second and a continuous mode of 2θ from 0° to 70° for data collection. The Debye-Scherer formula was used to calculate the crystallite sizes of untreated TiO_2 and coupled TiO_2/WO_3 nanocomposite following the formula below.

$$D = k\lambda / \beta \cos \Theta$$

In which: D is the crystallite size (nm)
k = crystallite shape factor (0.9)
β = Full width at half maximum (FWHM) in radians
λ = X-ray wavelength (nm)

Shimadzu IRAffinity-1S attenuated total reflection Fourier transform infrared (ATR-FTIR) spectrophotometer operated at ambient temperature and wavelength range of 4000 - 600 cm^{-1} was applied. Each spectrum constituted average of 20 scans with a resolution of 8 cm^{-1}. The ATR crystal was thoroughly cleaned with 100% ethanol, and the anvil lowered before applying the sample for measurements and collection of the characteristic spectra.

The textural properties of coupled titanium (IV) oxide composites were examined using a Micromeritics 3FLEX sorptometer and N_2 gas as a sorbate at 77.5 K. Samples were outgassed for 16 hours at 230° C, prior to analysis, while specific surface area (SSA) was calculated using the Brunauer-Emmett-Teller (BET) method. The nitrogen uptake at almost saturation pressure was used to calculate the pore volumes, whereas the volume and surface area of the micropores were determined using t-plot analysis.

The band gap of the unmodified titanium (IV) oxide and the coupled TiO_2/WO_3 nanocomposite was measured using a UV-Vis spectrometer. A sample paste was made by dissolving 0.5 g of each sample in isopropanol and distilled water. On a clear glass slide, duplicate screen prints of each sample were applied, and a Lab Tech open air furnace was used to anneal the samples. The temperature of the furnace was programmed from 100 ℃ and increased by 100º every 10 minutes until it reached 500 ℃, where it stabilized and allowed stay two hours. The annealed films were run on a UV-Vis spectrometer of the PerkinElmer Lambda 25 using the parameters given in Table 1.

Table 1. UV-Vis Instrumental Parameters

Instrumental Parameters	Values
Wavelength range	200 - 1100 nm
Data interval	1 nm
Spectral band width	1 nm
Scan speed	480 scans

To determine the composite nanoparticles' photocatalytic activity and effectiveness as a visible light water purification medium was carried out using a PerkinElmer UV-Vis spectrometer Lambda 25, to trace progress of photocatalytic breakdown of methylene blue by measuring the absorbance of solutions at 663.9 nm.

2.4. Analysis of photocatalytic activity of coupled TiO_2 -WO_3 nanocomposites

We evaluated photocatalytic activity of TiO_2-WO_3 nanocomposites on degradation of recalcitrant organic compounds using methylene blue (MeB) as a model compound. Experiments were conducted at room temperature under the influence of visible light by reacting 50 mL of 20 mg/L MeB with 1 g/L photocatalyst (TiO_2-WO_3) for 30 minutes in the dark (15). The mixture was swirled on magnetic stirrer to achieve equilibrium between the dye molecules and the photocatalyst surface, remove self-decomposing methylene blue molecules and pre-made charge carriers from ambient light sources [16]. 5 mL aliquot of the initial sample solution was placed into a beaker, and illuminated with visible light using a Phillips 8W white light lamp (WLL) placed 4 cm from the solution. The process was repeated every 30 minutes and centrifuged at 2000 rpm for 5 minutes. PerkinElmer UV-Vis spectrometer Lambda 25 was used to determine the absorbance of the supernatant at 663.9 nm. Photocatalyst solutions of varying concentrations of 2 g/L, 3 g/L, 4 g/L, and 5 g/L were used in the experiment to evaluate the effects of photocatalyst loading. Using the most effective catalyst dose, the pH of the solutions was also set between 2 and 12. To calculate the effectiveness of MeB's decomposition, the following equation was used:

Efficiency of MeB decomposition (%)

$$\frac{(Co - C)}{Co} * 100 \quad \text{or} \quad \frac{Ao - A)}{Ao} * 100$$

Where:

Co = initial MeB concentration

C = MeB concentration that varies over time

Ao = initial MeB absorbance

A = Time-dependent MeB absorbance

2.5. Degradation of methylene blue

Aliquots amounting 5 mL each was drawn from a solution of MeB every 30 minutes for a period of three hours. The solutions were centrifuged at 1500 rpm for 15 minutes, dichromate technique was employed following closed reflux colorimetric method to monitor the level of mineralization in supernatant liquid [17]. The percentage mineralization in the aliquots was calculated using a graph of Chemical Oxygen Demand (COD) removal vs irradiation time.

2.6 Reusability of titanium (IV) oxide - tungsten (VI) oxide

Recyclability experiment was conducted to ascertain the stability of the coupled TiO_2/WO_3 nanocomposite. Four cycles of treatment were carried out using the same TiO_2-WO_3 photocatalyst in the subsequently, while fresh solutions of equimolar concentrations of MeB was applied in each cycle. Recovery of the photocatalyst for reuse followed vacuum filtration through 0.45 µm membrane, distilled water washing, two hours of 200 °C drying, and subsequent photocatalyst reactivation.

3. Results and Discussion

3.1 Fourier Transform Infrared analysis

Figure 3 displays the FTIR spectra of coupled TiO_2-WO_3, unmodified TiO_2, and unmodified WO_3. TiO_2 exhibited four distinct absorption peaks in the FTIR spectrum, at 615 cm^{-1}, 1400 cm^{-1}, 1627 cm^{-1}, and 2348 cm^{-1} as illustrated in Figure 3.

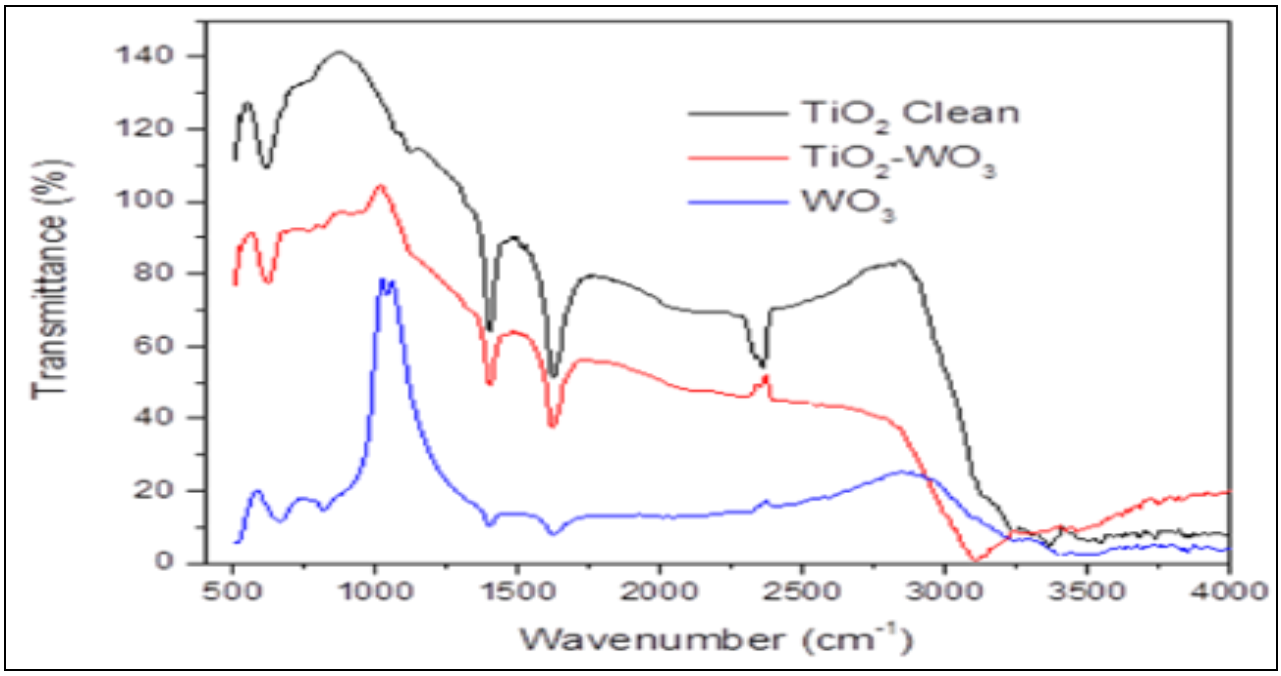

Figure 3. Fourier Transform Infrared Spectra of TiO_2, WO_3, TiO_2-WO_3

The peak at 615 cm^{-1} is caused by strong Ti-O and Ti-O-Ti bond stretching vibrations [18]. The molecularly adsorbed water molecule's O-H bending and the surface hydroxyl group's stretching vibration [19]. The 600–1000 cm^{-1} range of absorption values indicate a multitude

of stretching modes of O-W-O in the crystal lattice of WO_3 [20]. Despite the fact that WO_3 exhibited peaks at 662 cm^{-1}, 822 cm^{-1}, 1400 cm^{-1}, and 1627 cm^{-1}, in contrast to 1400 cm^{-1} and 1627 cm^{-1}, that reflects the adsorbed water O-H bending modes [21]. The TiO_2-WO_3 had absorption peaks in their FTIR spectra at 620 cm^{-1}, 1400 cm^{-1}, 1629 cm^{-1}, and 3108 cm^{-1}.

3.2 Analysis via X-ray Diffraction

X-ray diffraction patterns of unaltered titanium dioxide and coupled TiO_2-WO_3 nanocomposites are shown in Figures 4 and 5. Pronounced diffraction peaks observed at $2\theta = 25.4^O$, 37.86^O, 48.2^O, 53.88^O, and 62.8^O shown in the XRD spectra reflect the pattern for TiO_2 associated with the anatase crystalline phase's (101), (004), (200), (105), (211), and (220) planes [22]; [23]. The spectra revealed a tetragonal structure and which matched the standard spectrum (ICDD card 21-1272). TiO_2's characteristic diffraction peaks could still be seen in TiO_2-WO_3 composites, but they widened and gradually lost intensity as tungsten (VI) oxide (WO_3) content increased, suggesting that TiO_2 growth in the mixed oxide may have been hampered [24]. This suggests that the crystal structure of TiO_2 may have been impacted by the introduction of WO_3 when combined with TiO_2. Calcining at 575 °C showed the existence of only one phase, the tetragonal anatase structure, which is consistent with what is reported in literature, that only one crystalline phase exists between 500 - 600 °C [25].

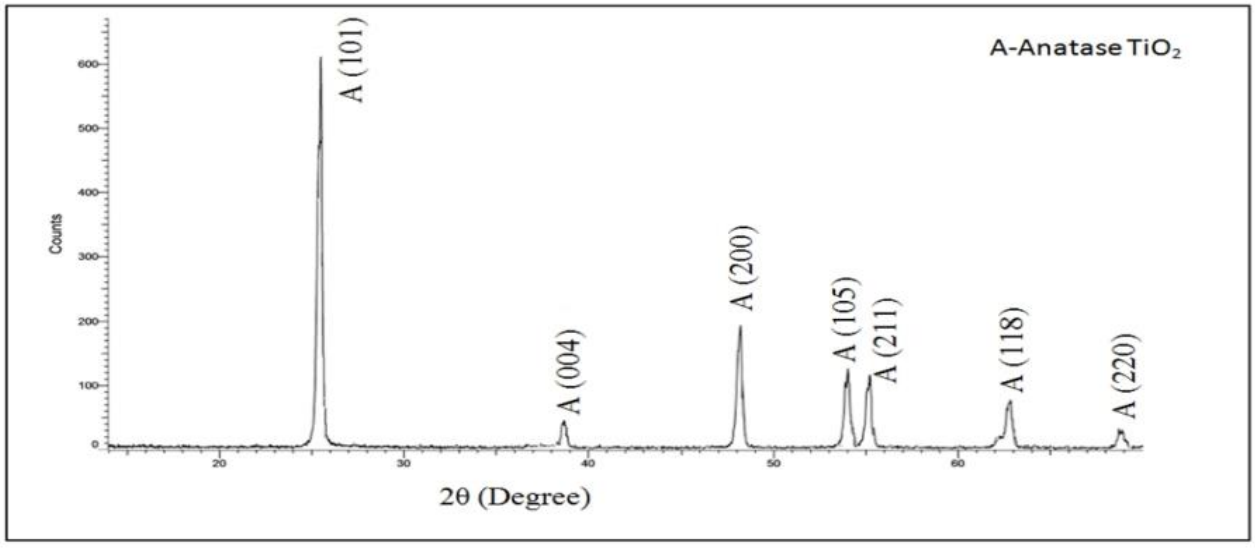

Figure 4. X-ray diffractograms for titanium (IV) oxide

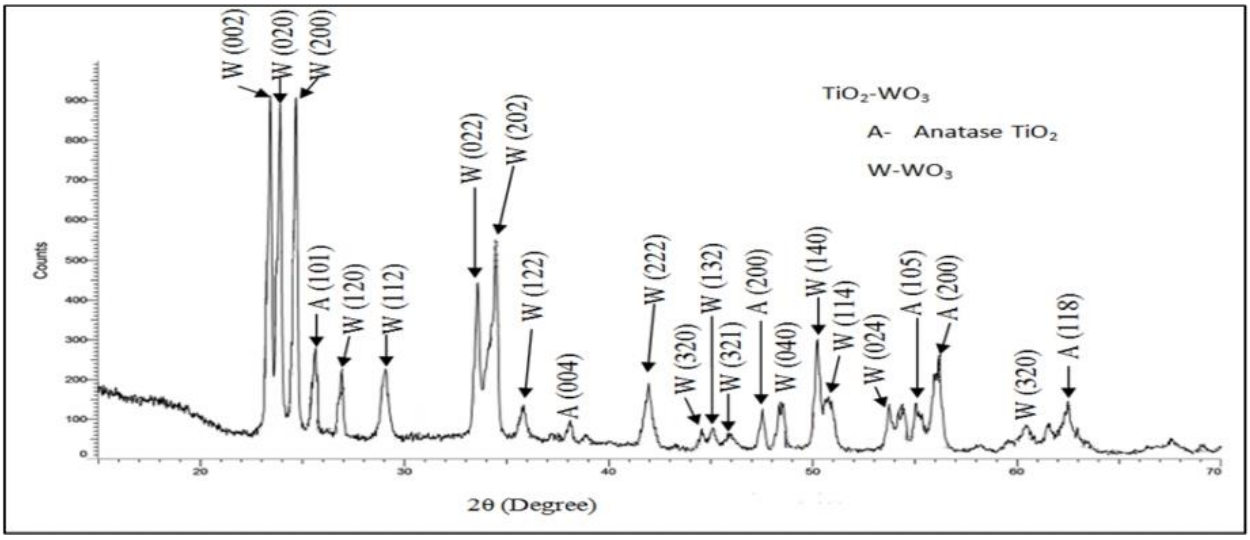

Figure 5. X-ray diffractogram for titanium (IV) oxide - tungsten (VI) oxide nanocomposites

XRD diffractograms of the coupled TiO_2-WO_3 nanocomposite revealed the presence of two crystal phases. Using the Eva software, the phases, shapes, and crystal characteristics of each nanocomposite were identified as shown in Table 2.

Table 2. Information on XRD diffractograms of the titanium (IV) oxide - tungsten (VI) oxide nanocomposites

Photocatalyst	Phases	Shape	Crystal Parameters		
			a	b	c
TiO_2-WO_3	Anatase	Tetragonal	3.730	3.730	9.370
	WO_3	Triclinic	7.280	7.480	3.820

When unmodified TiO_2 (22.2) is changed to modified TiO_2, i.e. TiO_2-WO_3 (56.7 nm), there was an increase in crystallite size, according to the findings in Table 3. The size of the crystallites grew. This means that coupling increases the number of active sites available for adsorption and photocatalytic surface reactions. This increase could also be ascribed to WO_3 clustering on the surface of TiO_2.

3.3. Brunauer-Emmet-Teller analysis

The nanocomposites were degassed using Micrometrics Smart VacPrep equipment for 16 hours at 503K. Nitrogen adsorption data at 77.5 K was used to assess the specific surface area and distribution of pore sizes using the Micromeritics 3 Flex Surface Characterization BET analyzer. Figure 6 shows a typical curve for adsorption on a non-porous powder with a diameter larger than the micropores depicted as a graph [26]. TiO_2-WO_3 nanoparticles were found to have 50 nm pore size and a specific surface area of 4.685 m^2/g. These values are smaller than those previously reported for TiO_2-WO_3 nanoparticles created using the sol gel method and Doctor blade technic [8]; [9]; [10], but larger than the sonochemical approach [11].

The resulting isotherm belongs to Type III of BET isotherms, since the isotherms for the adsorption and desorption curves coincide [23]. The curve also shows formation of a multilayer. Because there is no asymptote in the curve, and no monolayer formed. Adsorbed molecules are crowded on the surface of a non-porous substance, demonstrating the relative weakness of the adsorbent-adsorbate interactions. The nanocomposite has a multimodal pore size distribution as shown Figure 7, with a main peak located between 20 and 100, this is equivalent to a pore size of 50 nm.

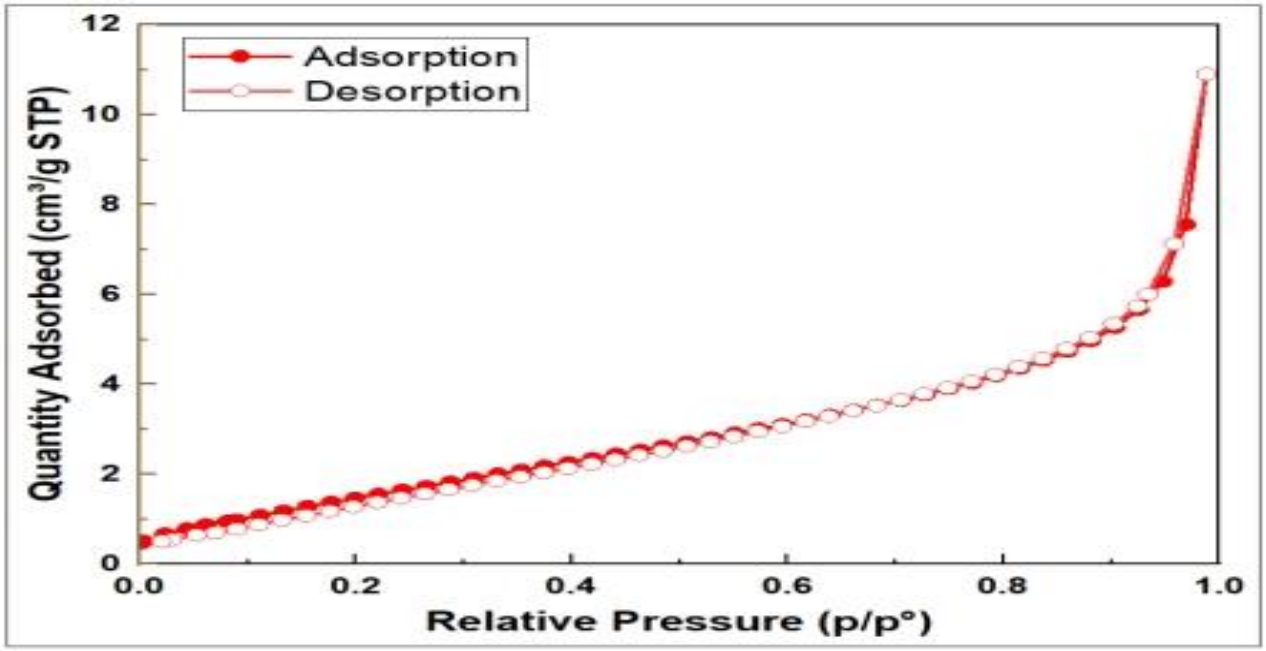

Figure 6. Titanium (IV) oxide - tungsten (VI) oxide BET isotherm

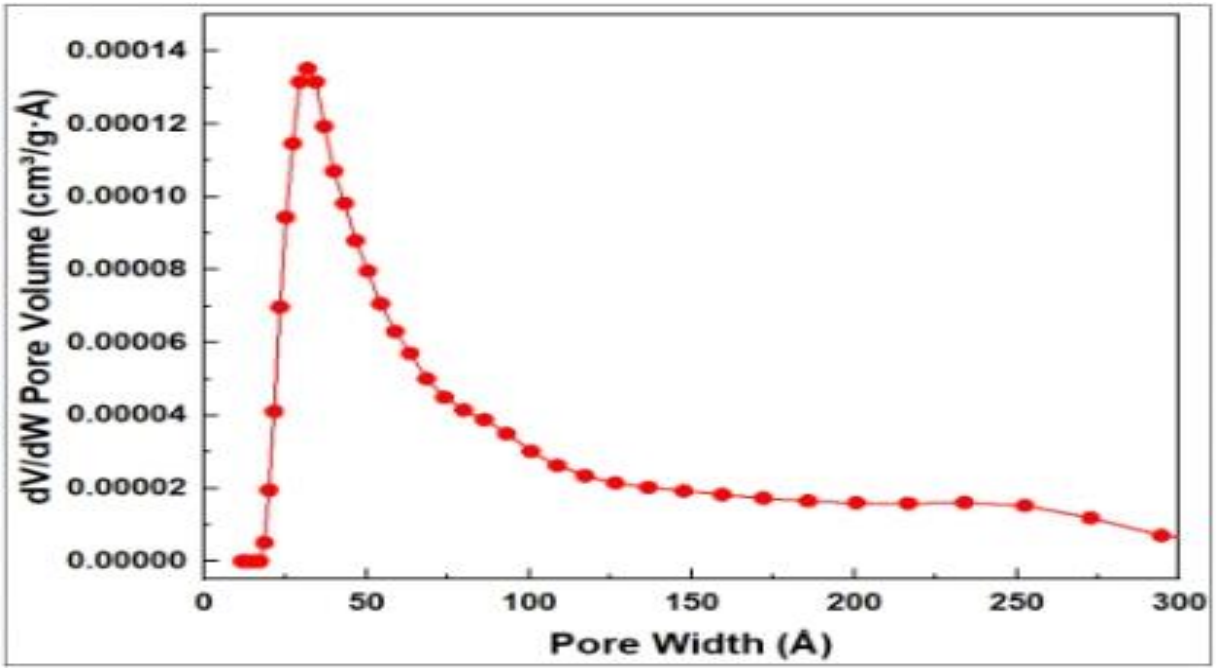

Figure 7. Titanium (IV) oxide - tungsten (VI) oxide pore size dispersion

3.4 Determination of band gap

Extrapolations in Figures 8 and 9 show that the modified TiO_2-WO_3 composites had a lower band gap energy (3.213 eV) than TiO_2 (3.317 eV). This demonstrates that the spectrum sensitivity of titanium (IV) oxide has been extended from the ultra violet to visible region when TiO_2 was combined with WO_3.

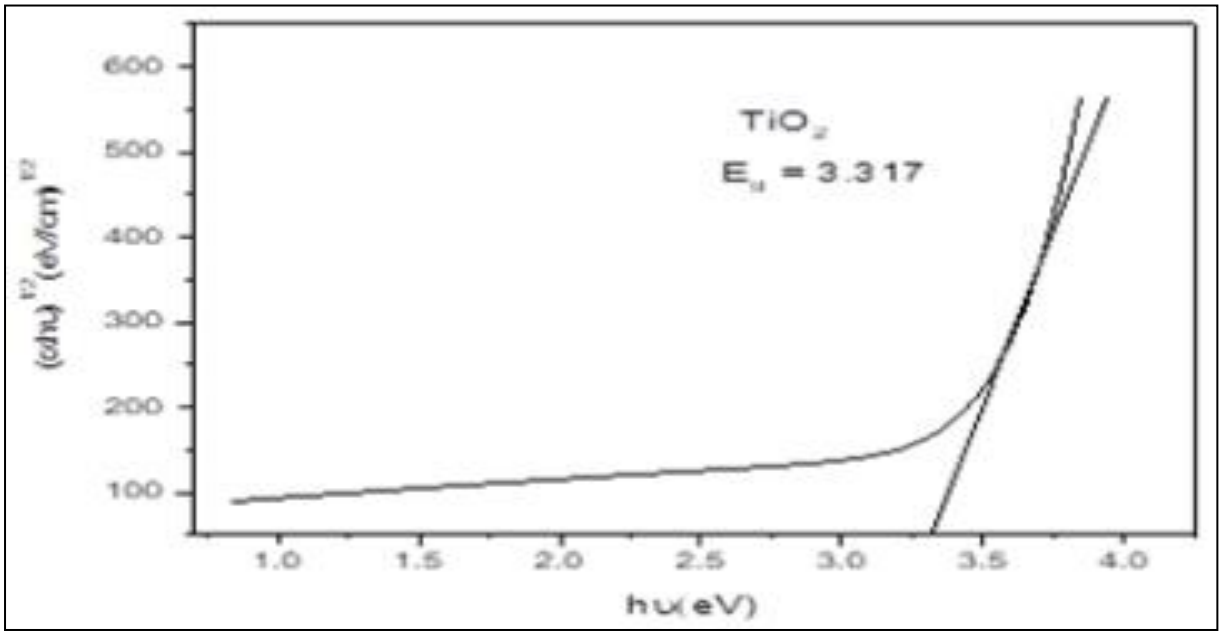

Figure 8. Band gap for titanium (IV) Oxide

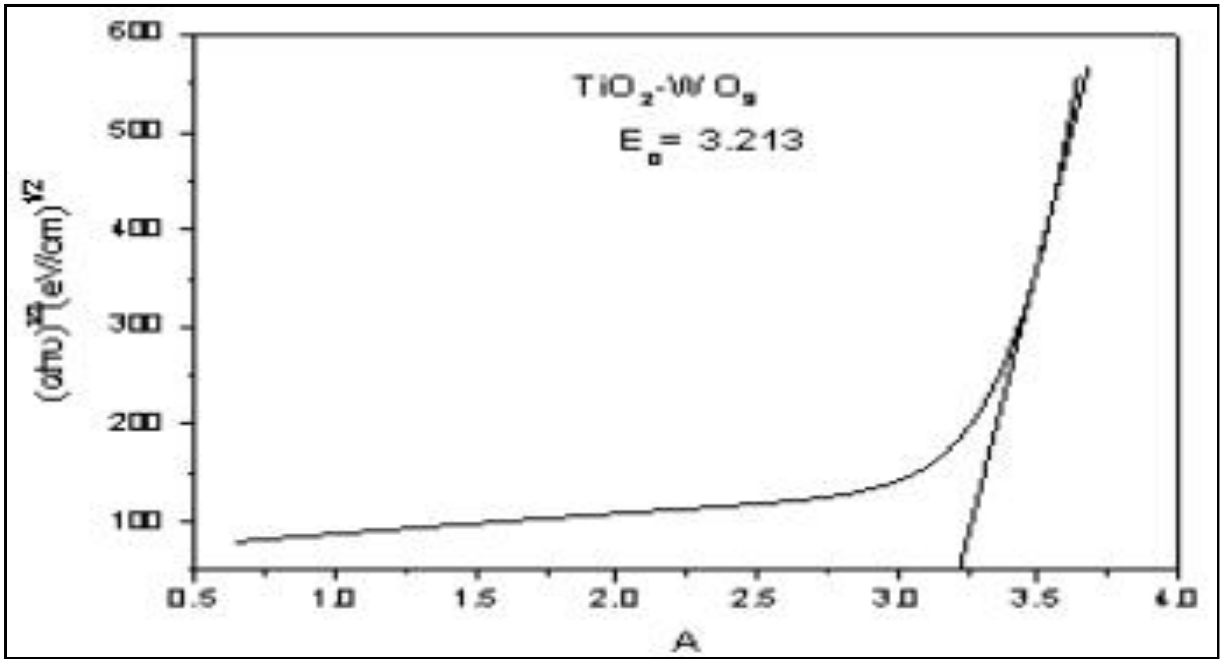

Figure 9. Band gap for titanium (IV) oxide - tungsten (VI) oxide

3.5. Titanium (IV) oxide - tungsten (VI) oxide nanocomposite's photocatalytic activity

Under visible light irradiation, the produced coupled TiO_2 nanocomposite was examined for methylene blue (MeB) degradation characterized by decolorization of the solution and

reduction in absorbances. The results of the impact of concentration, catalyst loading, nanocomposite ratio, surface area, and pH are discussed and illustrated in Figures 10, 11, 12, 13, and 14 below.

3.5.1. Concentration effect

The following solutions of methylene blue were used to measure the effect of concentration: 10, 15, 20, 25, and 30 milligrams per litre, while keeping the catalyst loading constant. Degradation efficiency decreased as concentration MeB dye increased in the solution (Figure 10).

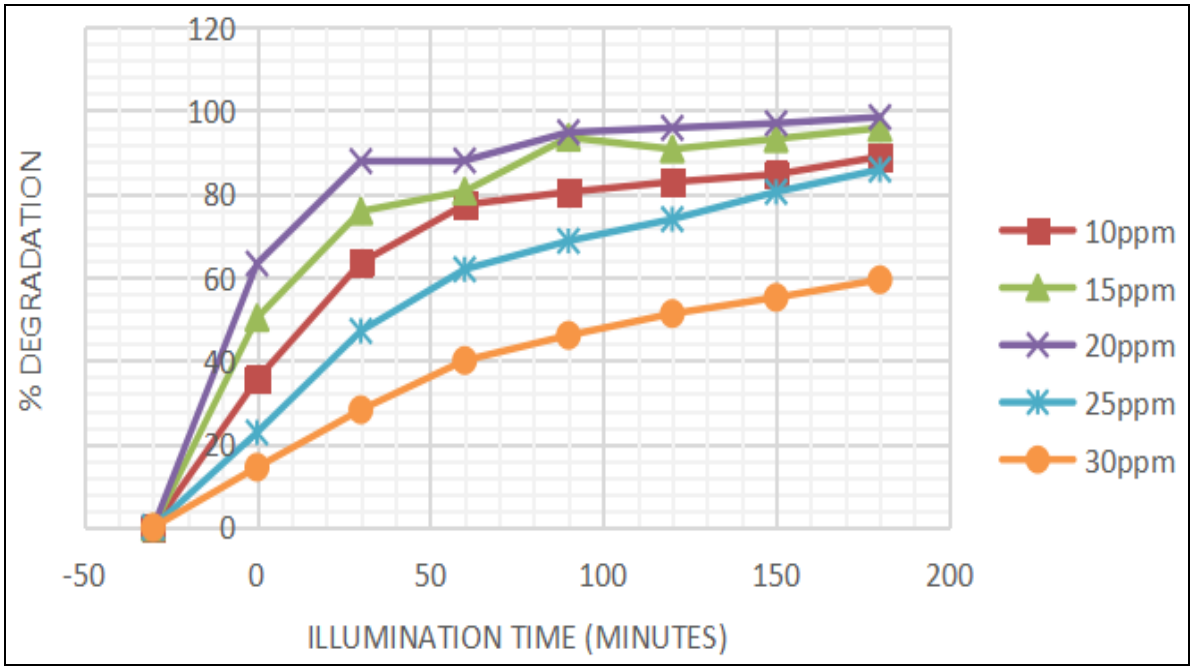

Figure 10. Effect of methylene blue dye concentration

This could be attributed to the fact that hydroxyl free radicals are produced on the photocatalyst surface and interact with adsorbed MeB molecules to cause degradation. Hence, when the dye concentration exceeded 20 mg/L, the molecules obstructed the active sites of the catalyst, resulting into lower rate of degradation [27].

3.5.2. Catalyst load

The impact of catalytic dosage was evaluated within the concentration range between 0.05 g and 0.25 g with a dye concentration of 20 mg/L. The best degradation performance was observed with catalytic dosage of 0.25 g, while mass greater than 0.25 g turned the solution turbid which not only prevented light penetrating, but also increased dispersed of particles and light scattering (Figure 11). As a consequence of higher scattering of light, the amount of visible light absorbed decreased as well as production of free radicals, which ultimately slowed the overall the rate of degradation.

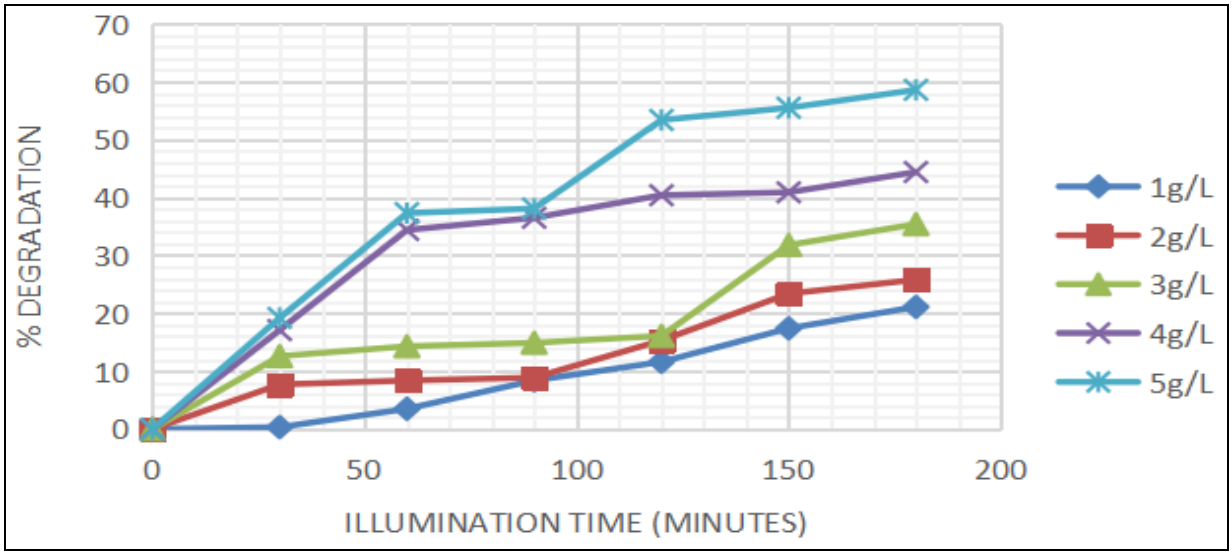

Figure 11. Effect of catalyst loading

3.5.3. Mole ratio of semiconductors

The performance of the coupled photocatalyst in degradation of MeB was evaluated against solutions containing only WO_3 or TiO_2. In the mole ratio of 1:1 for TiO_2:WO_3, the nanocomposite achieved 87.8% MeB degradation in 60 minutes, demonstrating outstanding performance. The degradation capacity for the same reaction following mole ratios of 1:4 and 4:1 was 21% and 6%, respectively, suggesting that an excess of the oxide did not couple. Due to TiO_2's inherent inefficiency under visible light, photocatalytic activity was weak in absence of coupling [28] due to the large band gap of TiO_2 which prevents the excitation of electrons from the valence band to the conduction band. Alternatively, excessive WO_3 exhibited a high rate of electron/hole recombination, resulting in a poor degradation of MeB. Hence under suitable conditions enhanced degradation of the organic dye can be accomplished by expanding the spectral range of TiO_2's photocatalytic response from the ultra violet to the visible region through coupling; which also decreases the recombination of the electron/hole pairs, lengthens their lives, and extends the lifetime of the electron/hole pairs themselves. The large band gap prevents excitation of electrons from the valence band to the conduction band [29].

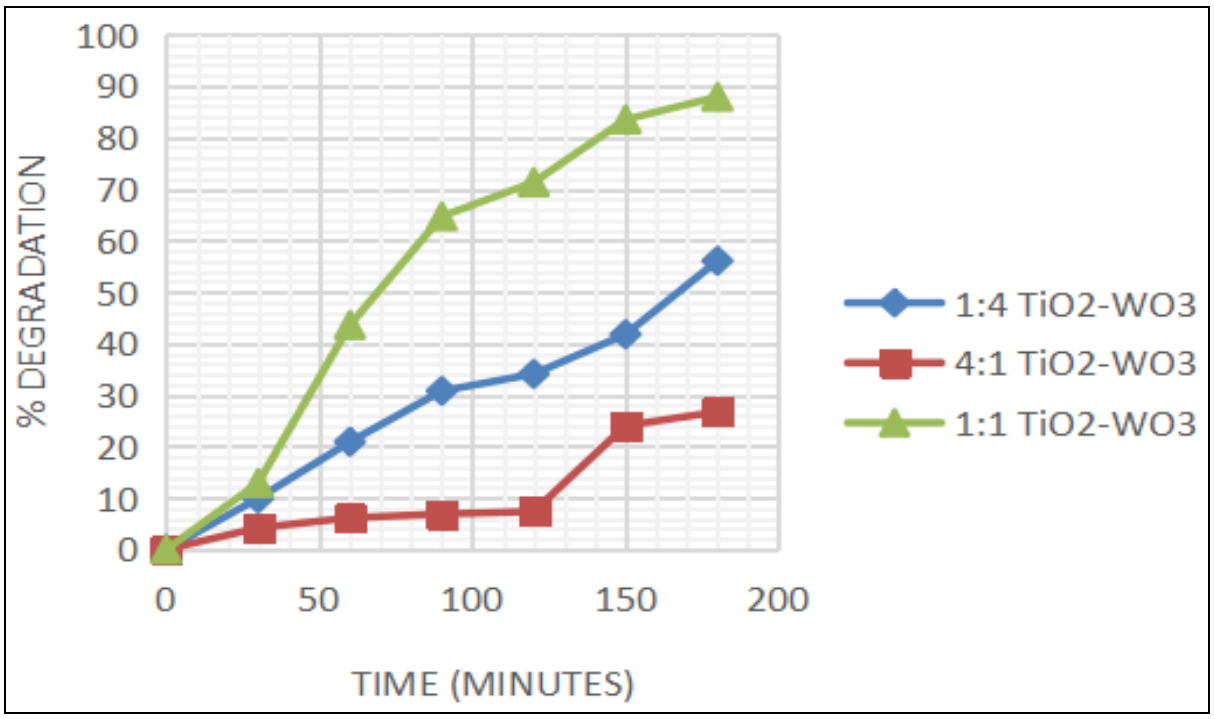

Figure 12. Effect of nanocomposite ratio

3.5.4. Effect of pH on photocatalytic degradation

At pH 12, high concentration of hydroxide ions in aqueous solution favour the formation of hydroxyl radicals, which react with adsorbed methylene blue (MeB) enhancing degradation and decolourisation of the later (Figure 13). Hence pH 12 was the optimal pH for methylene blue degradation degraded under the experimental conditions achieved. The drift approach revealed that the TiO_2-WO_3 nanoparticles' surface was negatively charged at pH 12 since the pH zero-point charge (pHpzc) was pH 6.2. The percentage of degradation investigated for pH 2 was slow at the beginning but gradually increased to a maximum of 90% at after 180 minutes. At pH < pHpzc, one would anticipate electrostatic repulsive interactions between the cationic methylene blue and the surface of TiO_2-WO_3 composites, since the adsorbent's surface was positively charged, and two cations are present in solution, MeB^+ and H^+ were both are vying for the adsorbent surface [30].

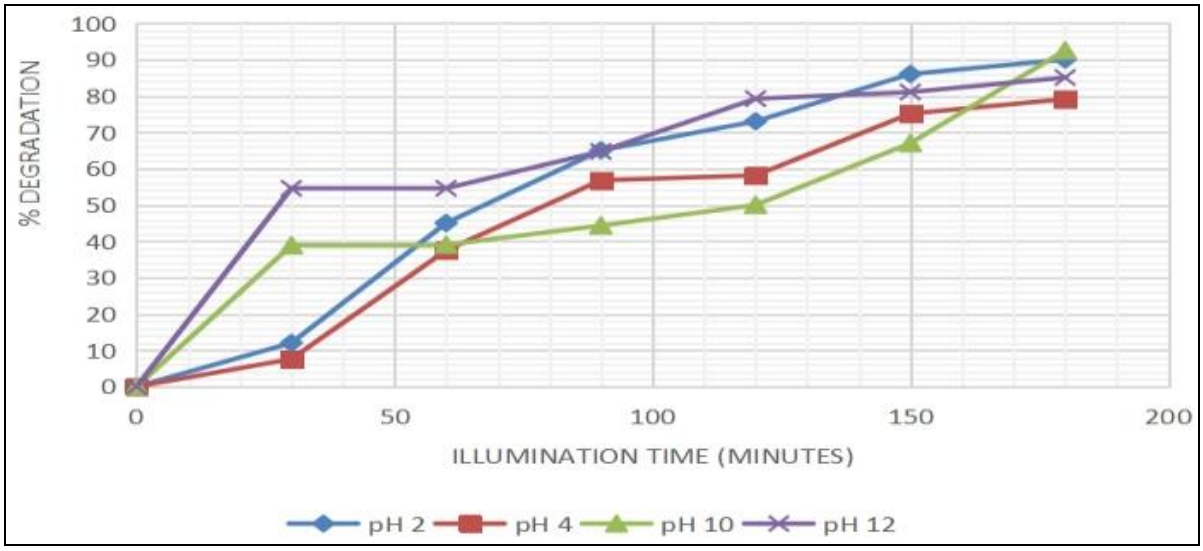

Figure 13. Effect of pH

3.5.5. Methylene Blue Degradation

A closed reflux colorimetric approach by chemical oxygen demand (COD) method was used to track degrdation of MeB dye in the aqueous solution. Data collected showed a decrease in the amount of organic matter created during MeB breakdown, which correlates to a greater percentage of COD being reduced. The results demonstrate obtained demonstrated that degradation of MeB occurred under the influence of visible light up to 86% reduction of COD in 3 hours (Figure 14).

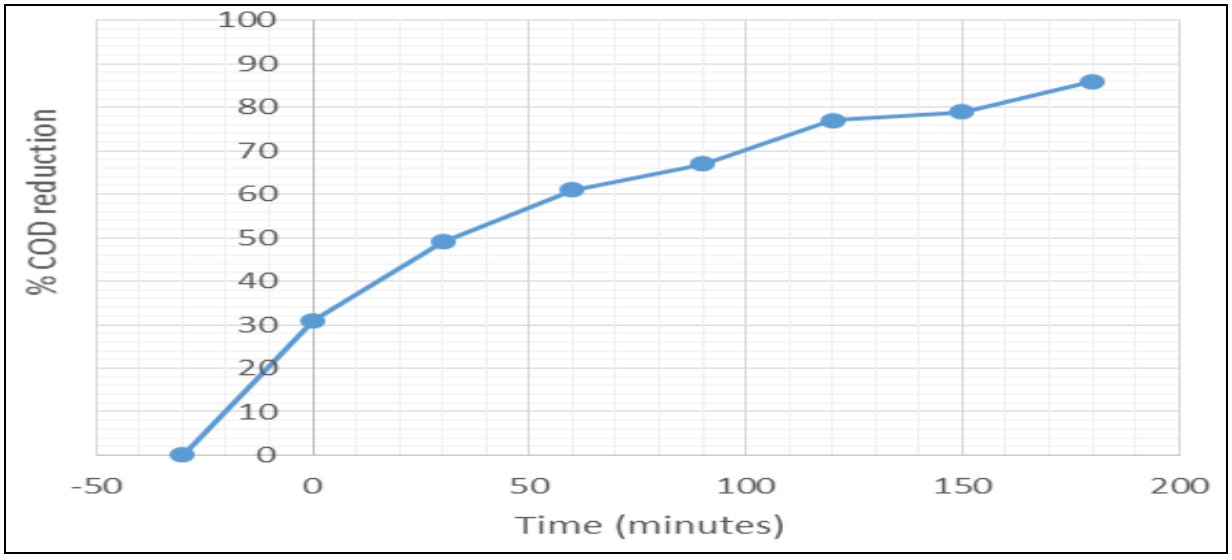

Figure 14. Reduction in chemical oxygen demand

3.5.7. Reusability of the photocatalyst

Evaluation of recyclability of the coupled TiO_2 nanocomposite was conducted by studying MeB degradation using the same photocatalyst in four different cycles of three hours each. Each cycle was followed by a regeneration of the photocatalyst by soaking for two hours in

isopropanol, vacuum filtering with 0.45 µm membrane filter membrane, washing with distilled water followed by two hours drying at 200 °C. Fresh MeB solution was used for each cycle to allow determination of removal efficiency. The proportion of MeB degraded decreased after each cycle, which was attributed partly to the loss of photocatalyst's weight after each recovery. The proportion of MeB degraded in respective cycles followed 93%, 90% 88% and 87% for cycles 1, 2, 3 and 4 respectively (Figure 15). The drop in percentage of MeB degraded in subsequent cycles could be due to reduction in surface area, a drop in the number of active sites for degradation of MeB, as well as formation of an inactive film on the catalyst surface. Photocatalytic activities and doping effects of metals have been reported in other studies [31, 32].

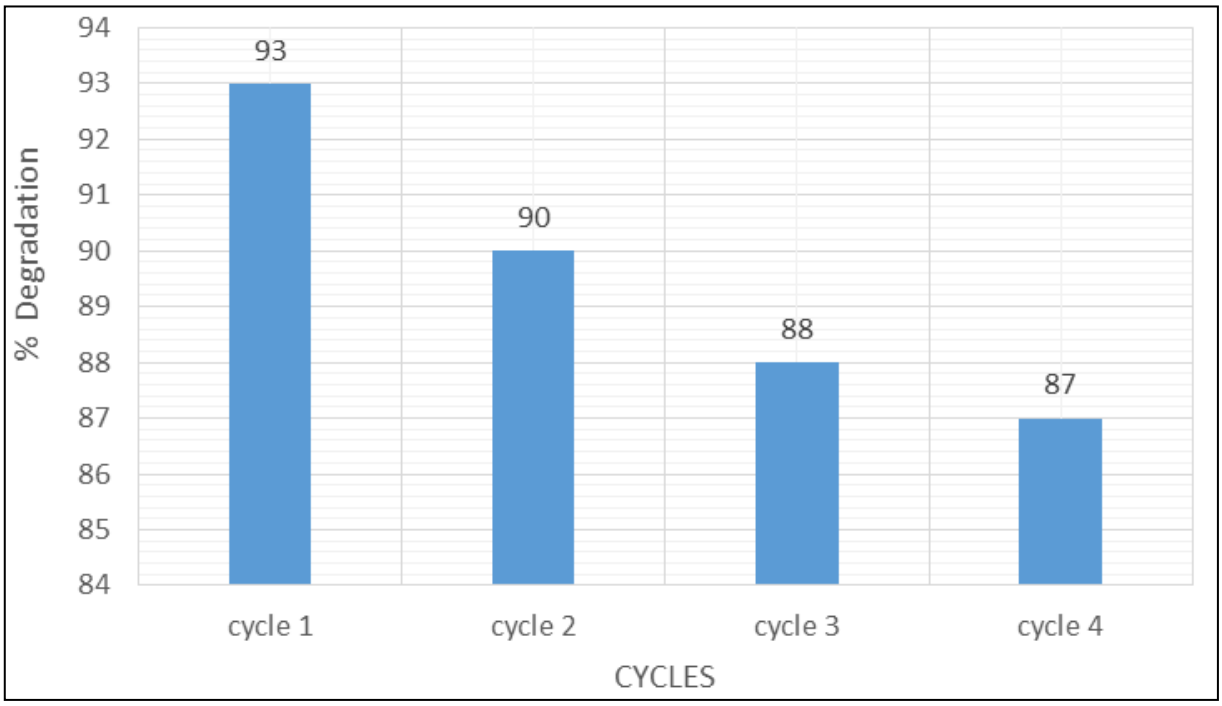

Figure 15. Titanium (IV) oxide - tungsten (VI) oxide photocatalyst reusability

4. Conclusion

A TiO_2-WO_3 nano-catalyst composite was synthesized under ambient temperature and pressure conditions, establishing a heterojunction that reduced the bandgap of TiO_2 from 3.317 eV to 3.213 eV, enabling a spectral response in the visible light region. Under optimal conditions, which included a catalyst dosage of 5g/L with a mole ratio of 1:1 TiO_2-WO_3, and a methylene blue solution concentration of 20 mg/L at pH 2 and pH 12, degradation of methylene blue reached a maximum of 90% at pH 2 and 87.8% at pH 12. The recyclability of the TiO_2-WO_3 nanocomposite, tested with fresh 20 mg/L methylene blue samples over four subsequent reuse cycles, maintained over 85% photocatalytic efficiency. These results indicate that the synthesized titanium dioxide coupled with tungsten trioxide nanocomposite has potential applications in the photocatalytic degradation of recalcitrant organic pollutants

in household water derived from diverse sources, namely, a lake, river, borehole, spring and a dam.

Disclosure statement

None of the writers have disclosed any conflicts of interest.

Acknowledgements

The DAAD and NRF financed this study.

References

[1] Ameta, R., Sharma, S., Sharma, S., & Gorana, Y. (2015). Visible light induced photocatalytic degradation of toluidine blue-O by using molybdenum doped titanium dioxide. *Eur. J. Adv. Eng. Technol*, *2*(8), 95-99.

[2] [2] Fayiga, A. O., Ipinmoroti, M. O., & Chirenje, T. (2018). Environmental pollution in Africa. *Environment, Development and Sustainability*, *20*(1), 41–73. https://doi.org/10.1007/s10668-016-9894-4

[3] Wang, C., Shi, Z., Peng, L., He, W., Li, B., & Li, K. (2017). Preparation of carbon foam-loaded nano-TiO_2 photocatalyst and its degradation on methyl orange. *Surfaces and Interfaces*, *7*, 116–124. https://doi.org/10.1016/j.surfin.2017.03.007

[4] Mahlambi, M. M., Ngila, C. J., & Mamba, B. B. (2015). Recent Developments in Environmental Photocatalytic Degradation of Organic Pollutants: The Case of Titanium Dioxide Nanoparticles—A Review. *Journal of Nanomaterials*, *2015*, 1–29. https://doi.org/10.1155/2015/790173

[5] Kushwaha, S., Soni, H., Ageetha, V., & Padmaja, P. (2016). An Insight into the Production, Characterization, and Mechanisms of Action of Low-Cost Adsorbents for Removal of Organics from Aqueous Solution. *Critical Reviews in Environmental Science and Technology*, *43*(5), 443–549. https://doi.org/10.1080/10643389.2011.604263

[6] Yang, C., Dong, W., Cui, G., Zhao, Y., Shi, X., Xia, X., Tang, B., & Wang, W. (2017). Highly- efficient photocatalytic degradation of methylene blue by PoPD-modified TiO_2 nanocomposites due to photosensitization-synergetic effect of TiO_2 with PoPD. *Scientific Reports*, *7*(1). https://doi.org/10.1038/s41598-017-04398-x

[7] Haghighi, M., & Nikoofar, K. (2016). Nano TiO_2/SiO_2: An efficient and reusable catalyst for the synthesis of oxindole derivatives. *Journal of Saudi Chemical Society*, *20*(1), 101–106. https://doi.org/10.1016/j.jscs.2014.09.002

[8] Khan, A., Alam, U., Ali, D., & Muneer, M. (2018). Visible-Light Induced Simultaneous Oxidation of Methyl Orange and Reduction of Cr (VI) with Fe (III)-Grafted K_2 Ti_6 O_{13} Photocatalyst. *Chemistry Select*, *3*(27), 7906–7912. https://doi.org/10.1002/slct.201800982

[9] Koohestani, H. (2019). Characterization of TiO_2/WO_3 composite produced with recycled WO_3 nanoparticles from WNiFe alloy. *Materials Chemistry and Physics*, *229*, 251-256. https://doi.org/10.1016/j.matchemphys.2019.03.027

[10] Riboni, F., Dozzi, M. V., Paganini, M. C., Giamello, E., & Selli, E. (2017). Photocatalytic activity of TiO_2-WO_3 mixed oxides in formic acid oxidation. *Catalysis Today*, *287*, 176-181. https://doi.org/10.1016/j.cattod.2016.12.031

[11] Giuffrida, F., Calcagno, L., Pezzotti Escobar, G., & Zimbone, M. (2023). Photocatalytic Efficiency of TiO_2/Fe_2O_3 and TiO_2/WO_3 Nanocomposites. *Crystals*, *13*(3), 372. https://doi.org/10.3390/cryst13030372

[12] Mullamuri, B., Mosali, V. S. S., Manseed, H., Majety, S. S., & Chandu, B. (2021). Photocatalytic Activity of Heavy Metal Doped CdS Nanoparticles Synthesized by Using Ocimum sanctum Leaf Extract. *Biointerface Research in Applied Chemistry*, *11*(5), 12547–12559. https://doi.org/10.33263/briac115.1254712559

[13] Kuo, C.-Y., Jheng, H.-K., & Syu, S.-E. (2021). *Effect of non-metal doping on the photocatalytic activity of titanium dioxide on the photodegradation of aqueous bisphenol A*. Retrieved April 5, 2022, from https://www.tandfonline.com/doi/epub/10.1080/09593330.

[14] Lee, Y., Kim, E., Park, Y., Kim, J., Ryu, W., Rho, J., & Kim, K. (2018). Photodeposited metal-semiconductor nanocomposites and their applications. *Journal of Materiomics*, *4*(2), 83–94. https://doi.org/10.1016/j.jmat.2018.01.004

[15] Wang, W., Huang, G., Yu, J. C., & Wong, P. K. (2015). Advances in photocatalytic disinfection of bacteria: Development of photocatalysts and mechanisms. *Journal of Environmental Sciences*, *34*, 232–247. https://doi.org/10.1016/j.jes.2015.05.003

[16] Sabbaghi, S., & Doraghi, F. (2016). Photo-Catalytic Degradation of Methylene Blue by ZnO/SnO_2 Nanocomposite. *Journal of Water and Environmental Nanotechnology*, *1*(1), 27–34. https://doi.org/10.7508/jwent.2016.01.004

[17] Zheng, G., Wang, J., Liu, H., Murugadoss, V., Zu, G., Che, H., & Guo, Z. (2019). Tungsten oxide nanostructures and nanocomposites for photoelectrochemical water splitting. *Nanoscale*, *11*(41), 18968-18994. https://doi.org/https://doi.org/10.1039/c9nr03474a

[18] Zarrabi, M., Haghighi, M., & Alizadeh, R. (2019). Enhanced sono-dispersion of Bi_5O_{7I} and Bi_2ClHO_3 oxides over ZnO used as nanophotocatalyst in solar-light-driven removal of methylene blue from water. *Journal of Photochemistry and Photobiology A: Chemistry*, *370*,105–116. https://doi.org/10.1016/j.jphotochem.2018.10.007

[19] Haw, C., Chiu, W., Abdul Rahman, S., Khiew, P., Radiman, S., Abdul Shukor, R., Hamid, M. A. A., & Ghazali, N. (2016). The design of new magnetic-photocatalyst nanocomposites ($CoFe_2O_4$–TiO_2) as smart nanomaterials for recyclable-photocatalysis applications. *New Journal of Chemistry*, *40*(2), 1124–1136. https://doi.org/10.1039/C5NJ02496J

[20] Zupančič, G. D., & Roš, M. (2012). Determination of Chemical Oxygen Demand in Substrates from Anaerobic Treatment of Solid Organic Waste. *Waste and Biomass Valorization*, *3*(1), 89–98. https://doi.org/10.1007/s12649-011-9087-1

[21] Rimoldi, L., Giordana, A., Cerrato, G., Falletta, E., & Meroni, D. (2019). Insights on the photocatalytic degradation processes supported by TiO_2/WO_3 systems. The case of ethanol and tetracycline. *Catalysis Today*, *328*, 210–215. https://doi.org/10.1016/j.cattod.2018.11.035

[22] Ouda, A. A., Mohamad Alosfur, F. K., Ridha, N. J., Abud, S. H., Umran, N. M., Al-aaraji, H. H., & Madlool, R. A. (2018). Facile method to synthesis of anatase TiO_2 nanorods. *Journal of Physics: Conference Series*, *1032*, 012038.https://doi.org/10.1088/1742-6596/1032/1/012038

[23] Hammad, A., El-Shazly, A., & Haitham, E. (2018). Effect of WO_3 Morphological Structure on its Photoelectrochemical Properties. *International Journal of Electrochemical Science*, 362–372. https://doi.org/10.20964/2018.01.32

[24] Ahmadi, M., Ramezani Motlagh, H., Jaafarzadeh, N., Mostoufi, A., Saeedi, R., Barzegar, G., & Jorfi, S. (2017). Enhanced photocatalytic degradation of tetracycline and real pharmaceutical wastewater using MWCNT/TiO_2 nano-composite. *Journal of Environmental Management*, *186*, 55–63. https://doi.org/10.1016/j.jenvman.2016.09.088

[25] Arce-Sarria, A., Machuca-Martínez, F., Bustillo-Lecompte, C., Hernández-Ramírez, A.,& Colina-Márquez, J. (2018). Degradation and loss of antibacterial activity of commercial amoxicillin with TiO_2/WO_3-assisted solar photocatalysis. *Catalysts*, *8*(6), https://doi.org/10.3390/catal8060222

[26] Thommes, M., Kaneko, K., Neimark, A. V., Olivier, J. P., Rodriguez-Reinoso, F.,Rouquerol, J., & Sing, K. S. W. (2015). Physisorption of gases, with special reference to the evaluation of surface area and pore size distribution (IUPAC Technical Report). *Pure and Applied Chemistry*, *87*(9–10), 1051–1069. https://doi.org/10.1515/pac-2014-1117

[27] Alkaykh, S., Mbarek, A., & Ali-Shattle, E. (2020). *Photocatalytic degradation of methylene blue dye in aqueous solution by $MnTiO_3$ nanoparticles under sunlight irradiation | Elsevier Enhanced Reader*. https://doi.org/10.1016/j.heliyon.2020.e03663

[28] Grandcolas, M., Cottineau, T., Louvet, A., Keller, N., & Keller, V. (2013). Solar light-activated photocatalytic degradation of gas phase diethylsulfide on WO_3-modified TiO_2 nanotubes. *Applied Catalysis B: Environmental*, *138–139*, 128–140. https://doi.org/10.1016/j.apcatb.2013.02.041

[29] Li, R., Li, T., & Zhou, Q. (2020). Impact of Titanium Dioxide (TiO_2) Modification on Its Application to Pollution Treatment—A Review. *Catalysts*, *10*(7), 804. https://doi.org/10.3390/catal1007080

[30] Geçgel, Ü., Özcan, G., & Gürpınar, G. Ç. (2012). Removal of Methylene Blue from Aqueous Solution by Activated Carbon Prepared from Pea Shells (Pisum sativum). *Journal of Chemistry*, *2013*. https://doi.org/10.1155/2013/614083

[31] Byrne, C., Subramanian, G., & Pillai, S. C. (2018). Recent advances in photocatalysis for environmental applications. *Journal of Environmental Chemical Engineering*, *6*(3), 3531–3555. https://doi.org/10.1016/j.jece.2017.07.080

[32] Mugunthan, E., Saidutta, M. B., & Jagadeeshbabu, P. E. (2019).Photocatalytic activity of ZnO-WO_3 for diclofenac degradation under visible light irradiation. *Journal of Photochemistry and Photobiology A: Chemistry*, *383*, 111993. https://doi.org/10.1016/j.jphotochem.2019.111993